



Universiteit
Leiden
The Netherlands

Nonlinear optical studies of single gold nanoparticles

Dijk, M.A. van

Citation

Dijk, M. A. van. (2007, October 17). *Nonlinear optical studies of single gold nanoparticles*. *Casimir PhD Series*. Retrieved from <https://hdl.handle.net/1887/12380>

Version: Corrected Publisher's Version

License: [Licence agreement concerning inclusion of doctoral thesis in the Institutional Repository of the University of Leiden](#)

Downloaded from: <https://hdl.handle.net/1887/12380>

Note: To cite this publication please use the final published version (if applicable).

2

Third-harmonic generation

2.1 Introduction

Optical signals from single nano-objects open new windows for studies at nanometer scales in fields as diverse as material science and cell biology. Cleared from ensemble averaging, distributions and time-dependent fluctuations stand out. Simpler pictures of molecular processes emerge from first-hand comparison to theoretical models. Early work has concentrated on aromatic dye molecules, whose fluorescence can be detected with a very high signal-to-background ratio [22]. Their applications as labels for single biomolecules are considerably limited by photobleaching. This irreversible destruction of the molecule forces the experimentalist to change molecule and to hark back to statistics, thereby losing part of the advantages of single-molecule methods. Semiconductor nanocrystals, which resist bleaching for longer times, have recently been introduced as labels [74]. The random interruption of their luminescence by long off-times is, however, a serious drawback for many applications. Tracking biomolecules requires chemically and photochemically stable labels, ideally no larger than a few nanometers. Noble metals, in particular gold, strongly interact with light while being chemically inert. Because they resist high illumination levels and don't saturate, and because they can be attached to biomolecules, as is currently done in electron microscopy, gold nanoparticles would be appealing optical labels.

Being bridges between molecules and solids, metal nanoparticles and colloids show fascinating size and confinement effects. Their linear and nonlin-

ear optical properties are the subject of active research [28, 75, 76, 77]. Much of the current work bears on large ensembles of nanoparticles in gas phase, solid matrices, or liquid solutions. In such bulk samples, the properties of interest can be obscured by the distribution of sizes, and in the case of liquid suspensions, by aggregates, which can easily dominate the signal of isolated colloids. The need for small-sized labels has rekindled interest in the photoluminescence of noble metal particles [54, 55, 75]. However, the luminescence yield of all except the smallest metal clusters is weak, and strongly depends on surface states and defects. Therefore, more reliable optical contrast mechanisms are desirable. Scattered laser light enables tracking of gold particles larger than 100 nm in biological media, where a high background arises from other scatterers. Such large labels, however, may hamper the functions of tagged biomolecules in real cells. Interferometric detection of laser heating was recently proposed as a two-color contrast mechanism to image gold nanoparticles as small as a few nanometers [68]. Other nonlinear processes may offer simpler ways to optically detect metal nanoparticles. Multiphoton processes are expected to be amplified by enhanced electric fields within, or in the vicinity of, metal particles, and may provide sufficient contrast against background from the surroundings.

The simplest nonlinear effect, second-harmonic generation (SHG), is forbidden for a perfect spherical particle much smaller than the wavelength. SHG will therefore strongly depend on defects, facets and other small deviations from the spherical shape. It will strongly vary from particle to particle, which is a drawback for labelling. In this chapter, we consider third-harmonic generation (THG, i.e. third-order hyper-Rayleigh scattering), which is allowed in all media, and requires only one pump color. Giving a specific signal for particles of a given size, THG can distinguish labels of different sizes. We have explored the strength of the THG signal of single gold particles in a confocal microscope, in view of its possible combination with THG in bio-imaging [6, 78].

2.2 Experimental method

In a THG experiment, we deal with a large spectral difference between fundamental and third harmonic. If the source at the fundamental frequency is a titanium:sapphire laser, for instance, the third harmonic lies in the deep ultraviolet (270 nm), where imaging is difficult and photodetection inefficient. Instead, we chose to use the signal beam of an optical-parametrical oscillator (OPO) at a wavelength of 1500 nm as the fundamental. The Mie frequency

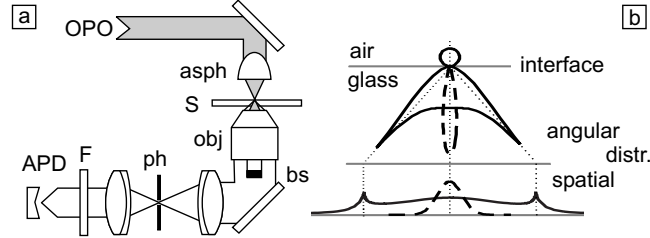


Figure 2.1: a) The central part of the experimental setup. The OPO signal beam (1500 nm) is focused by an aspheric lens **asph** (NA 0.65) on the sample **S**. The generated light is collected by an oil immersion objective **obj** (NA 1.4). The coherent background is suppressed by a beam stop **bs** and a pinhole **ph**. The filter **F** blocks the excitation light. b) Comparison of the angular emission pattern of a dipole (—) and the phase-matched coherent background (- -). The dipole points out of the paper plane.

of gold colloids with diameters lower than 100 nm (about 520–560 nm) is then close to resonance with the third harmonic, thus enhancing its generation [79]. The OPO produces nearly Fourier-limited pulses of about 1.2 ps width at a repetition rate of 76 MHz. This light is coupled into a home-built microscope (Fig. 2.1a). The sample is scanned by a piezo stage through the overlapping foci of an aspheric lens (excitation) and an oil immersion objective (detection). This way, both excitation and detection benefit from efficient optics. A confocal pinhole reduces the detection volume and a band-pass filter (510 ± 20 nm) allows only the third harmonic to reach the avalanche photodiode. The detection rate is recorded as a function of the position of the scanning piezo stage.

The samples are gold colloids (British Biocell International, EM.GC) of different diameters d (40, 50, 60, 80, 100, and 150 nm) spin-coated in a polymer solution (polyvinyl-alcohol, PVA, 10 g/l) on a clean glass cover slide. Special care was taken to avoid changes in the ionic strength of the solution which may cause aggregation of the colloids. We imaged mono-disperse samples and mixtures of two different diameters where the larger particles (100 or 150 nm) served as references.

Bulk THG cancels for a focused beam in massive materials because of the Gouy phase shift on both sides of the focus, but it still takes place in the vicinity of interfaces [80]. This background, which is several orders of magnitude higher than the THG from gold colloids, can be dramatically suppressed by exploiting the difference in angular THG emission patterns of the interface and of a single colloid (Fig. 2.1b). The interface THG-beam is created in a

2 Third-harmonic generation

coherent process in the direction of the exciting beam with one third of its numerical aperture (NA) [80]. The THG pattern from a colloid can be approximated by that of a dipole at the interface [81]. When the THG-beam is collimated by a high-NA objective, the outer parts of the parallel beam are dominated by colloid THG, and the interface THG can be blocked by a beam-stop in the center. In our case a beam-stop of 3.2 mm diameter transmits only about 10^{-5} of the interface THG but about 75 % of the colloid THG. This simple device reduced the coherent background THG below the dark count rate of the detector (40 cps).

2.3 Single gold nanoparticles

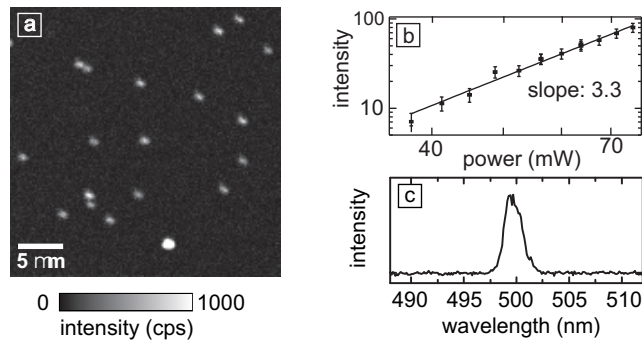


Figure 2.2: a) Raster-scanned image of colloids ($d = 100$ nm), 100 ms/pixel integration time, 75 mW excitation power; b) Excitation power dependence of the detected THG signal, measured on a single 100-nm colloid by fitting a 2D Gaussian to series of scans; c) Emission spectrum of a single 100-nm colloid. The full width at half maximum of the peak is 2 nm.

Figure 2.2a shows a $30 \times 30 \mu\text{m}$ raster scan of a sample obtained by spin-coating a solution of 100-nm colloids. In this image, several peaks with approximately the same height can be discerned. The signal shows clear signatures of third-harmonic generation: the emitted intensity has a third-power dependence on the excitation intensity (Fig. 2.2b) and the spectrum consists of a single narrow line (FWHM of 2 nm) centered around 500 nm, corresponding to three times the fundamental frequency (Fig. 2.2c). The time-dependence of the THG signal is constant over very long intervals, as shown the bottom panel of Fig. 2.3a. Outside the filter passband, the only detected emission is a second line centered around 750 nm, at twice the fundamental frequency (i.e., the second harmonic). As mentioned in the introduction, the

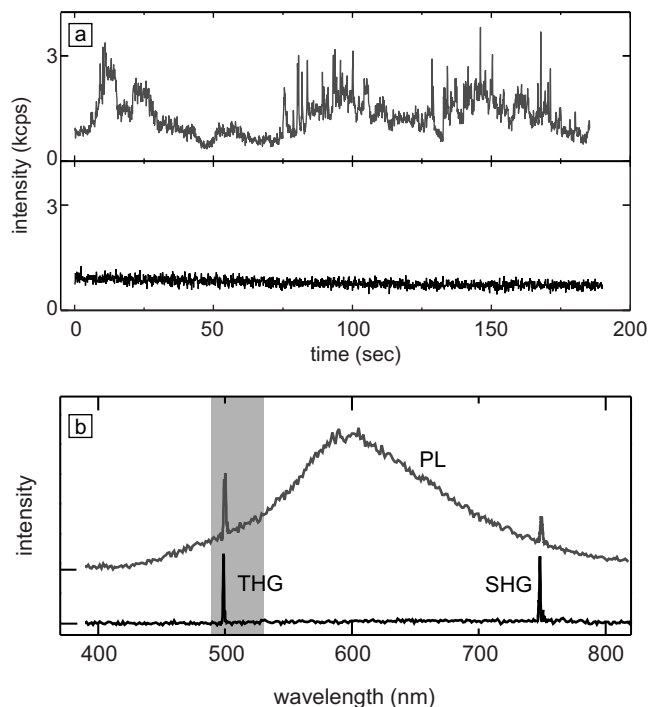


Figure 2.3: a) Time traces of two single 100-nm colloids; b) Emission spectra corresponding to the same two colloids. All colloids show THG and SHG, a small fraction of the colloids additionally show photoluminescence (PL, upper spectrum in b)) with a very irregular time dependence (upper timetrace in a)). Note the difference in SHG intensity between the two spectra, which points to the sensitivity of this signal to defects.

SHG line can be explained by defects in the colloid (e.g. deviations from a perfect sphere) or by an environment-broken symmetry (e.g., due to the air-glass interface). Since this line fell outside our detection window, it did not contribute to the confocal image (Fig. 2.3c, bottom spectrum).

The spot in the bottom center of Fig. 2.2a is much brighter than the others (it is saturated in the gray scale of Fig. 2.2a). Such "hot" colloids could be identified in the images by their high intensity. As can be seen at the top of Fig. 2.3b, the spectrum of a hot colloid contains, in addition to the THG and SHG lines, a broad peak centered around 600 nm, with a much higher integrated intensity. This photoluminescence spectrum has been previously observed under two-photon excitation by Beversluis et al. [53]. Most hot colloids presented extremely bright flares over microseconds to milliseconds (Fig. 2.3a), covering a large range of intensities (flickering), but we never

2 Third-harmonic generation

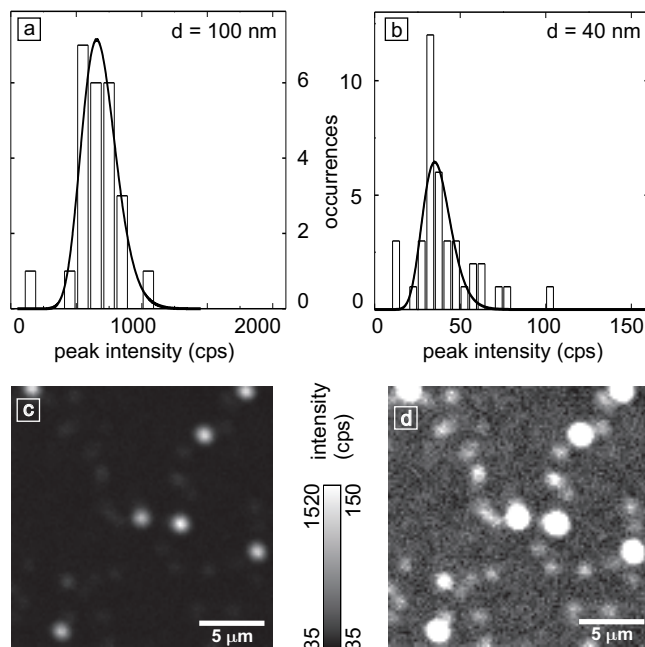


Figure 2.4: a,b) Histograms of the peak intensities above background for a pure 100-nm sample (a) and the 40-nm colloids of a mixed sample (b). The fit yields a relative diameter distribution $\Delta d/d$ of 7 % (100 nm) and 8 % (40 nm) which agree with the manufacturer's values (5 % and 6 %). c,d) Raster-scanned image of a mixture of 40-nm and 100-nm gold colloids (600 ms integration time). The same scan is shown with two different intensity scalings. In (d) the 100-nm colloids are saturated, but the 40-nm colloids appear above the background.

observed the clear on-off blinking of single molecules and nanocrystals. The hot colloids (in total 2 %) were left out of the THG analysis that follows.

Histograms of peak intensities of the THG from normal colloids were extracted from images in the following way. We filtered a copy of each image with a Gaussian correlation filter. All pixels above a certain threshold (70 cps) were found to cluster in spots. At these positions we fitted a Gaussian intensity distribution to the unfiltered data. We thus ended up with histograms of spot intensities above the background level. Two examples are shown in Fig. 2.4a and b. All the histograms show a monomodal Gaussian distribution with a significant offset from the background. This feature unambiguously discriminates a distribution of single objects from a distribution of aggregates with different sizes. The spots that fall into the lowest bins of each histogram are attributed to specks of dust or fluctuations in the background level that

triggered the fitting procedure. The histograms can be fitted assuming a normal size distribution and the size dependence discussed below. The resulting relative width $\Delta d/d$ matches the values of the manufacturer's test certificate. Fig. 2.4c and d shows the same scan of a 40 and 100-nm mixture in two different intensity gray scales. In Fig. 2.4d the 40-nm colloids appear above the background. This diameter of 40 nm was our detection limit (at 600 ms integration time) with a fundamental average intensity of 2 MW/cm² (peak intensity of 40 GW/cm²), which was limited by OPO output.

2.4 Size dependence

With increasing particle size, the third-harmonic signal increases as the square of the induced nonlinear dipole, which, for a cluster of independent molecules, would increase as their number. Thus, when the nonlinear susceptibility originates from *bound* electrons and is therefore a molecular, size-independent property, we expect a sixth-power dependence of the THG intensity on cluster diameter. Fig. 2.5 shows the average signal intensity for 6 sizes of particles, from 40 nm to 150 nm. The slope of the plot across the whole range is compatible with a third- to fourth-power dependence in diameter, and clearly deviates from a sixth power (for which the ratio of 40 nm to 150 nm colloid signal should be 14 times lower).

A metal's *free* electrons can lead to a size-dependent susceptibility. In an infinite metal bulk, free electrons perform exactly harmonic plasma oscillations. In nanoparticles, however, finite size and surfaces give rise to anharmonicity. Recently, Fomichev et al. [79, 82] have theoretically considered THG by plasma oscillations in a small conducting sphere, when the third harmonic is resonant with the plasmon frequency. For a neutral particle at high intensity, they predict a significant production of third harmonic, and a fourth-power dependence of the intensity on diameter. Their calculation is based on the slight deviation from a harmonic potential that the electron charge distribution experiences when it oscillates as a whole around the fixed ion distribution. In this model, THG can be seen as induced by the surface of the sphere. The induced dipole is therefore proportional to the area of the sphere rather than to its volume. This leads to a third-harmonic intensity varying as the fourth power of the diameter. The signal intensity we measure, taking our collection efficiency into account, is in good order-of-magnitude agreement with the formula of Ref. [79] for neutral particles, although we are in a regime of much lower intensities.

Note, however, that retardation effects lead to a significant change in the

2 Third-harmonic generation

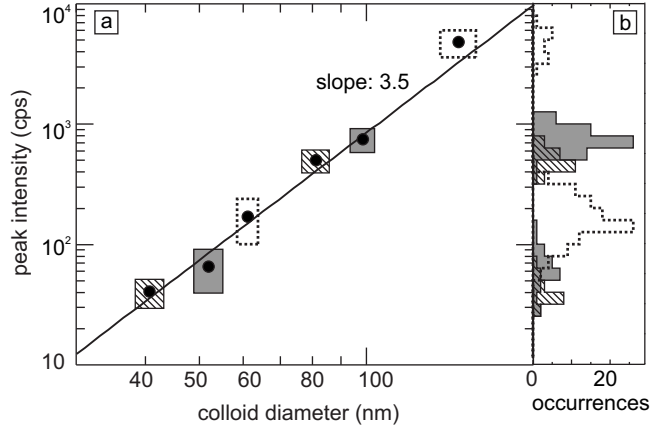


Figure 2.5: a) Size dependence of the THG signal of single gold colloids: mean values (black dots) of the obtained histograms shown in part (b). The boxes represent the error bars: The intensity error is estimated by the histogram standard deviation and the size error is the width of the size distribution as given in the manufacturer's test certificate. The data was fitted with a power law (black line). To correct for thermal drifts, the colloid samples were mixed with 100-nm colloids, used as references (150-nm colloids were taken as references for the 80-nm colloids). The excitation power was 68 mW, the integration time was 100 ms (600 ms for the 40-nm colloids).

absorption spectrum for colloids larger than about 50 nm. This gives an additional size-dependent factor in both the bound-electron and the free-electron model, which is difficult to estimate. The accurate calculation of the influence of retardation on the third-harmonic generation is computationally demanding and has, to our knowledge, only been done for the bound-electron case [83]. It is therefore desirable to measure THG from yet smaller individual colloids, where retardation is negligible. The 1-ps pulses of our current laser system limited us to 40-nm particles. With the 100-fs pulses of current commercial OPO's, and assuming the fourth-power to hold on for lower sizes, we estimate a signal-to-noise ratio of more than unity for 15-nm particles, with the present accumulation time of 600 ms.

2.5 Conclusion

We have demonstrated that single gold nanoparticles can be detected by third-harmonic generation. Peak-height histograms show that each spot in the image is produced by a single particle. In the present setup colloid sizes down to 40 nm are detectable, but the use of 100-fs pulses should allow us to

2.5 Conclusion

image 15 nm particles. Even if this limit would be hard to reach in a scattering medium such as a cell, and smaller labels can be detected with photothermal heterodyne detection [84], single particle spectroscopy through THG can be advantageous when combined with THG imaging [6]. The size-dependence of the THG signal would make it possible to distinguish labels of different sizes. Gold nanorods (elongated particles) might further increase the signal to volume ratio of the particles [77]. However, the absorption of water at 1500 nm must be taken into account for biological samples. In order to avoid attenuation of the fundamental power and heating problems, the sample thickness should not exceed some tens of micrometers, about the size of a cell.

We thank Dr. F. Kulzer for his help during early stages of this experiment.

